

Review

Recent Advances for Imidacloprid Detection Based on Functional Nanomaterials

Shu Chen ¹, Yawen Wang ², Xiuli Liu ² and Longhua Ding ^{2,*} ¹ School of Bioengineering, Shandong Polytechnic, Jinan 250104, China² Institute for Advanced Interdisciplinary Research, School of Chemistry and Chemical Engineering, University of Jinan, Jinan 250022, China

* Correspondence: bio_dinglh@ujn.edu.cn

Abstract: Imidacloprid (IMI) has been applied in agricultural production to prevent pests. It is vital to detect IMI residues with high sensitivity for food safety. In general, nanomaterials have driven the development of highly sensitive sensing platforms owing to their unique physical and chemical properties. Nanomaterials play important roles in the construction of high-performance sensors, mainly through sample pretreatment and purification, recognition molecules immobilization, signal amplification, and providing catalytic active sites. This review addresses the advances in IMI sensors based on the combination of nanomaterials and various analytical techniques. The design principles and performance of different chromatographic, electrochemical, and fabricated optical sensors coupled with nanomaterials are discussed. Finally, the challenges and prospects of sensors based on nanomaterials for IMI analysis have also been incorporated.

Keywords: imidacloprid; nanomaterials; chromatographic methods; electrochemical sensors; optical sensors



Citation: Chen, S.; Wang, Y.; Liu, X.; Ding, L. Recent Advances for Imidacloprid Detection Based on Functional Nanomaterials. *Chemosensors* **2023**, *11*, 300. <https://doi.org/10.3390/chemosensors11050300>

Academic Editor: Fabio Gosetti

Received: 6 April 2023

Revised: 5 May 2023

Accepted: 16 May 2023

Published: 18 May 2023



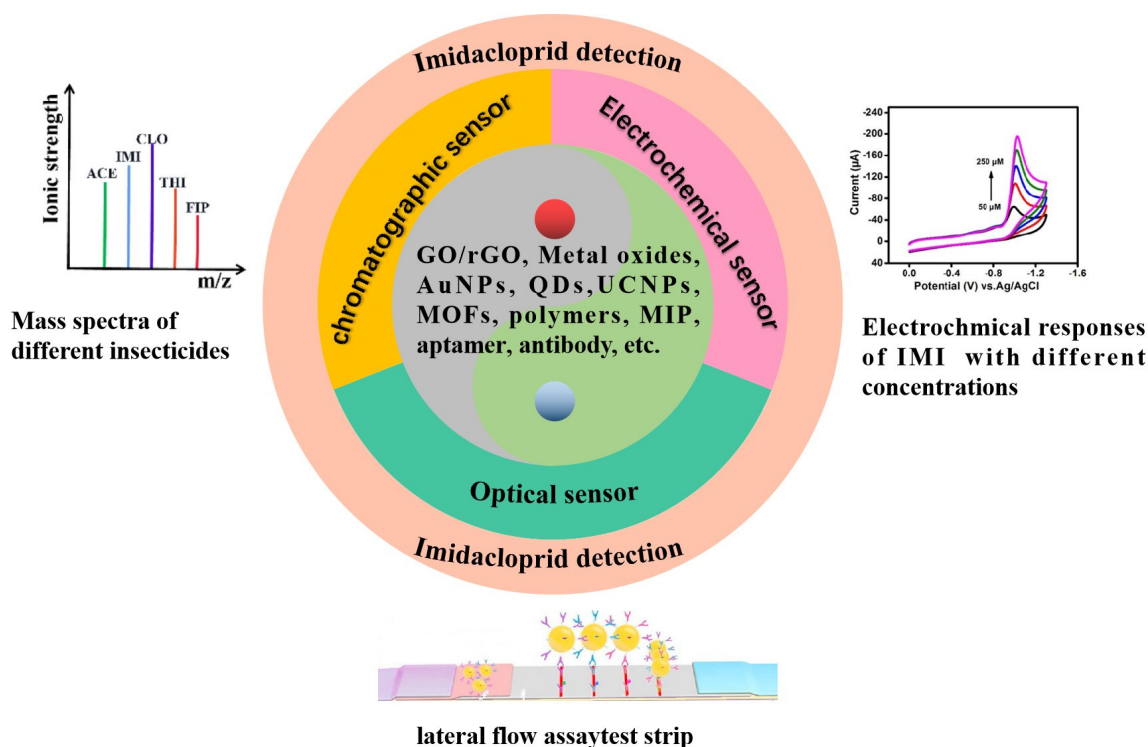
Copyright: © 2023 by the authors. Licensee MDPI, Basel, Switzerland. This article is an open access article distributed under the terms and conditions of the Creative Commons Attribution (CC BY) license (<https://creativecommons.org/licenses/by/4.0/>).

1. Introduction

In recent years, the market share of neonicotinoid pesticides has steadily increased in the global insecticide market because of their relative low toxicity to mammals but high activity against insects [1]. As a first-generation neonicotinoid pesticide, imidacloprid (IMI, 1-((6-Chloro-3-pyridinyl)methyl)-N-nitroimidazolidinimine) was first introduced in the 1990s. IMI is the largest-selling pesticide among neonicotinoid pesticides, and it is widely used for seed treatment in agriculture to protect crops from pests. It acts on the nicotinic acetylcholine receptor (nAChRs) by disturbing the central nervous systems of insects [2]. However, the long lifetime and high dose uses of IMI lead to large residues in environmental water, soil, and food, which could enter the human body through the food chain and pose a potential risk to human health [3–5]. This has led to some related laws being established to limit the maximum amount of IMI residue. For example, in 2018, the European Union banned the use of IMI [6]. The Chinese national standard GB 2763-2021 stipulated that the maximum residues of IMI in Chinese cabbage were 0.2 mg/kg [7]. Thus, it is particularly necessary to develop reliable methods for IMI residue detection.

Up until now, various analytical methods have been developed for pesticide detection, including chromatographic techniques, electrochemical methods, and optical methods. Each of them has its own advantages and disadvantages (discussed in detail in Part 3). For example, efficient sample pretreatment methods are required before chromatographic analysis [8]. The weaker electrochemical response of IMI on traditional bare electrodes results in low sensitivity. Introducing nanomaterials into these analytical techniques can overcome these shortcomings. With the advancement of nanotechnology and synthetic methodologies, various nanostructure materials (NMs), including carbon-base materials (graphene, carbon nanotubes, porous carbon, etc.), metal nanoparticles, metal oxides and

sulfides, upconverting nanoparticles, metal-organic frameworks (MOFs), conducting polymers, and their composites, have been designed and prepared [9–12]. These nanostructure materials possess excellent physicochemical and plasmonic properties owing to their small particle size and high surface area. These properties make them an essential part of the field of analytical techniques [13–16]. Nanomaterials play roles in sensor construction by enhancing catalytic activity, immobilizing biological entities (enzyme, antibody, aptamer, etc.), signal amplification, purification, exaction, and separation [17–21]. This review aims to cover the recent development of IMI sensors by combining these analytical techniques with various nanomaterials (Scheme 1).



Scheme 1. The analytical methods for IMI are based on various nanomaterials. Reproduced from [22–24] with permission from ACS and Elsevier.

2. The Metabolites of IMI

When pesticides are applied to crops, they are often converted into metabolites. In the case of IMI, the degradation of IMI produces several metabolites, including imidacloprid-olefin (IMI-olefin), urea-imidacloprid (IMI-urea), 6-chloronicotinic acid (6-CNA, or 6-chl), 5-hydroxy-imidacloprid (5-OH-IMI), desnitro-imidacloprid (DN-IMI), and nitro-methylene analogue (CH-IMI) [25–30], etc. Their chemical structures are shown in Figure 1. The metabolites produced by IMI are related to the environment, and they exhibit higher toxicity than IMI. For example, in casing soil during mushroom cultivation, the main metabolites were IMI-urea, IMI-olefin, and 6-CNA [31]. In honey, the concentrations of IMI-olefin (5.6 ng g^{-1}) and 5-OH-IMI (21.1 ng g^{-1}) were higher than those of IMI (0.8 ng g^{-1}) [32]. To make matters worse, the metabolites are more toxic than IMI itself. For example, IMI-olefin is twice as toxic as IMI [33]. Hence, the risk of IMI metabolites should be considered comprehensively when evaluating the harm of IMI.

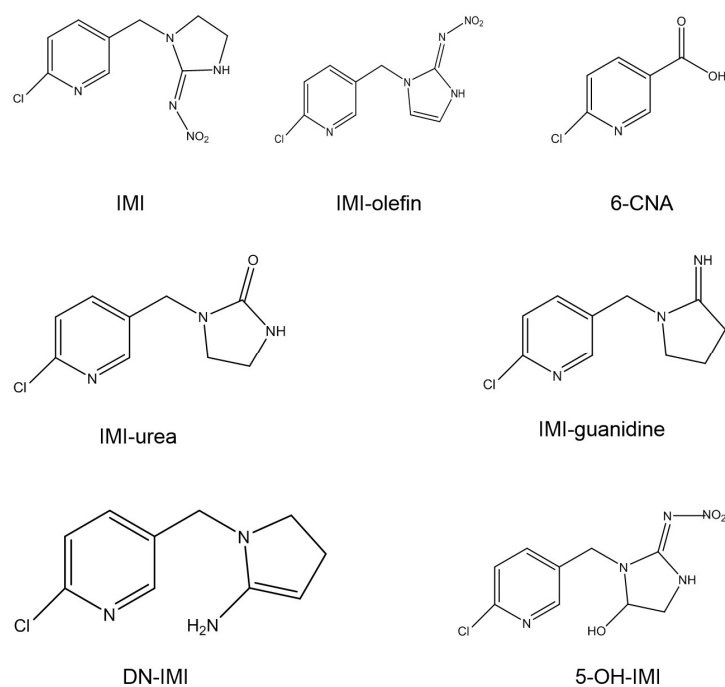


Figure 1. Chemical structures of IMI and its metabolites.

3. Detection Methods

3.1. Sample Pretreatment and Chromatographic Analysis

The traditional chromatographic methods, including gas chromatography (GC), high-performance liquid chromatography (HPLC), mass spectrometry (MS), gas chromatography-tandem mass spectrometry (GC-MS), high-performance liquid chromatography-tandem mass spectrometry (HPLC-MS), capillary electrophoresis-mass spectrometry (CE-MS), and ultraperformance liquid chromatography/tandem mass spectrometry (UPLC-MS/MS), can offer high accuracy and have been recognized as the gold standard for the detection of many organic analytes [34–37]. However, owing to the wide use of insecticides, they may exist in a variety of complex matrices, such as soil, food, Chinese medicine, etc., and the interferences in these matrices often affect the accuracy and sensitivity of detection [38]. Therefore, the determination of pesticide residues generally includes two steps: sample pretreatment and quantitative detection. Up to now, researchers have proposed versatile sample pretreatment methods to extract targets from different samples, such as solvent extraction, solid phase extraction (SPE), the QuEChERS method (the Quick, Easy, Cheap, Effective, Rugged, and Safe method), etc. [8,39–42]. Nanomaterials could be used for the extraction and enrichment of targets in complex matrices due to their small size, large specific surface area, and adjustable surface groups. At present, many types of nanomaterials have been used in sample pretreatment processes, such as carbon-based nanomaterials [43], polydopamine [44], MOFs [45,46], covalent organic frameworks (COFs) [47,48] and so on [49]. So far, researchers have realized that the determination of IMI in complex samples is based on pretreatment and chromatographic analysis (Table 1). For example, Xu et al. [50] proposed an UPLC-MS/MS method for IMI detection. Firstly, IMI was extracted with UiO-66-NH₂ as an adsorbent and acetonitrile as a desorption solution. Then, IMI was treated by UPLC with a gradient eluting procedure and identified by electrospray ionization (ESI) on a mass spectrometer. Moreover, this method successfully detected IMI in fruit samples with satisfactory recovery. Kharbouche et al. [51] applied a mesoporous material (MSU-1) as a sorbent to preconcentrate 218 pesticides in environmental waters and subsequently determine them by UPLC-MS/MS. Mou et al. [23] used nitrogen and sulfur co-doped carbon dots (N,S-CDs) as QuEChERS cleanup reagents in the complex samples and determined multiple pesticides with a portable mass spectrometer (μ -MS) (Figure 2). This method could achieve simultaneous detection of five kinds of pesticides. Besides,

the metabolites of IMI were measured mainly by chromatographic analysis. For instance, Sánchez-Hernández et al. [52] confirmed the existence of IMI and DN-IMI in honey and maize crop samples by LC/QTOF-MS analytical techniques.

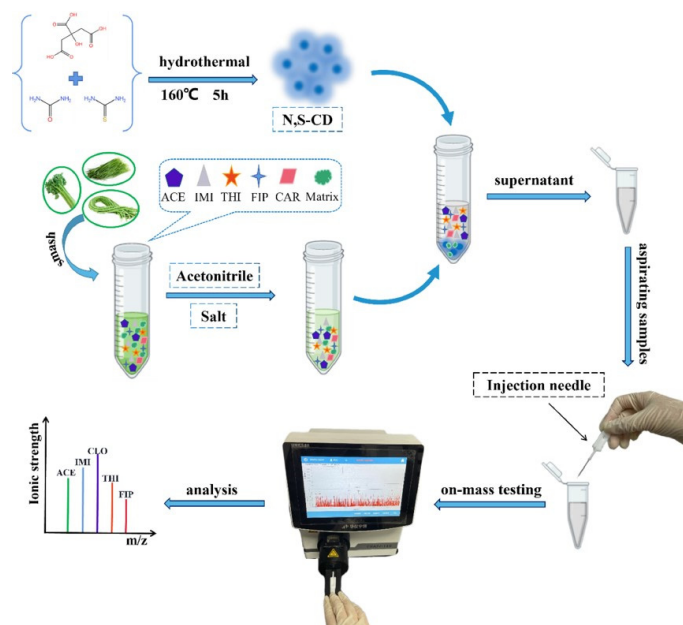


Figure 2. A diagram of the experimental procedure using N,S-CDs as the purification material. Reproduced from [23] with permission from Elsevier.

The quantitative detection of three metabolites, including IMI-olefin, 5-OH-IMI, and 6-chl, was achieved by Li et al. [53] using LC-QQQ/MS. The results showed that the residual concentration of these three metabolites varied according to vegetable tissue and exposure time. These results helped to understand the distribution of IMI and its metabolite residues in leaf vegetables. Moreover, these chromatographic methods exhibited excellent performance in the simultaneous detection of multiple analytes.

Table 1. Analytical performance of IMI detection based on chromatographic analysis.

Matrices	Sample Pretreatment	Analytical Technique	Recovery	LOD	Reference
fruit	SPE: UiO-66-NH ₂	UPLC-MS/MS	92.39%	0.04 µg L ⁻¹	[50]
groundwater	SPE: MSU-1	UPLC-MS/MS	80–86%	below 0.1 µg L ⁻¹	[51]
vegetables	QuEChERS: N,S-CD	µ-MS	82.2–109.7%	0.5–1.0 ng g ⁻¹	[23]
honey, tomato, lettuce and Chinese cabbage samples	SPE: ^a Fe ₃ O ₄ @Ph-HCP	HPLC	80.1–111%	0.30–0.67 ng g ⁻¹ (honey), 1–1.5 ng g ⁻¹ (tomato, lettuce and Chinese cabbage)	[54]
lemon juice, honey	SPE: ^b Rut-MOP	HPLC	82–118%	0.03–0.04 ng mL ⁻¹ (lemon juice), 2.5–3.0 ng g ⁻¹ (honey)	[55]
vegetable	^c MSPE: ^d (Fe ₃ O ₄ @COF-(NO ₂) ₂)	HPLC	81.7–103.5%	0.04 ng mL ⁻¹	[56]
cucumber, tomato and tap water	SPE: ^e TPN/Fe ₃ O ₄ NPs/GO	HPLC	91.2–102.4%	0.17 µg L ⁻¹	[57]
honey	anion exchanger- ^f DPX	LC-MS/MS	72–104%	1.5 µg kg ⁻¹	[34]
wheat samples	^g D-µSPE: ^h CNPC	HPLC	91–99%	0.056 µg Kg ⁻¹	[58]
wheat, rice and fruit	QuEChERS	LC-MS/MS	94.1–103.3%	-	[59]

^a Fe₃O₄@Ph-HCP: nitrogen-rich magnetic hypercrosslinked polymer; ^b Rut-MOP: hydroxyl-functional magnetic porous organic polymer; ^c MSPE: magnetic solid phase extraction; ^d (Fe₃O₄@COF-(NO₂)₂): magnetic covalent organic framework containing the nitro groups; ^e TPN/Fe₃O₄NPs/GO: triazine-based polymeric network modified magnetic nanoparticles/graphene oxide; ^f DPX: disposable pipette extraction; ^g D-µSPE: dispersive micro-solid phase extraction; ^h CNPC: CuO nanoplate-polyaniline composite.

3.2. Electrochemical Sensors

Recently, various electrochemical techniques have attracted much attention from researchers due to their numerous advantages, including high sensitivity, low cost, and easy preparation [60]. Hence, electrochemical methods have been used for constructing sensors for IMI. The electrochemical detection performance of IMI is mainly dependent on various electrode-modified materials, such as carbon composite, reduced graphene oxide, β -cyclodextrin, bismuth film, silica film, molecularly imprinted polymers, biological materials, and so on. There are mainly three electrochemical strategies for IMI detection: direct detection, indirect detection (electrochemical sensors based on MIPs and biometric recognition elements), and electrochemical ratio sensors.

3.2.1. Direct Electrochemical Detection

IMI is an electroactive molecule in which the nitro group can undergo two-electron or four-electron reduction on an electrode surface. The direct electrochemical reduction of IMI proceeded on various modified electrodes to improve the sensitivity (Table 2). β -cyclodextrin (β -CD) has a hydrophobic internal cavity and a hydrophilic external surface, which make it useful for capturing various molecules. Therefore, β -CD was extensively applied for sensor construction. For instance, Pereira [61] developed an electrochemical sensor for IMI based on β -CD film coated on a glass carbon electrode (GCE). The electrochemical performance of IMI on β -CD/GCE was better than that on bare GCE due to the encapsulating effect of β -CD for IMI. A variety of carbon materials, including carbon nanotubes, carbon paste, graphene oxide (GO) or reduced graphene oxide (rGO), etc., have excellent electrochemical properties and are widely used in electrochemical sensors. Urbanová et al. [62] constructed an IMI electrochemical sensor using GO-modified electrodes. The proposed sensor could detect IMI at 10–200 μ M with a limit of detection (LOD) of 8.3 μ M. Johnson et al. [63] established an electrochemical sensing platform for several neonicotinoids using laser-induced graphene (LIG) that was prepared by a scalable direct-write laser fabrication process. The LIG-based sensor exhibited a rapid response time (\sim 10 s) and excellent performance for IMI detection with a LOD of 384 nM. The composite composed of CD and carbon also acted as electrode-modified materials for IMI reduction. Zhao et al. [64] fabricated an electrochemical sensor using rGO/CD-modified GCE (Figure 3a). They found that rGO/ α -CD/GCE possessed the best analytical performance than other composites (rGO/ β -CD and rGO/ γ -CD) owing to the good supramolecular recognition of α -CD toward IMI. In addition, electrochemically reduced GO (E-rGO) was time-saving and cost-effective compared with rGO prepared by wet-chemical synthesis. The obtained E-rGO/ α -CD/GCE displayed a low LOD of 23 nM with a wider linear range of 0.5–40 μ M. Finally, this new sensor could detect IMI in brown rice with satisfactory recoveries. Our group [10] developed an electrochemical sensor for IMI based on raffia-derived porous carbon/polyaniline composite modified GCE (PRC@PANI/GCE). The PRC@PANI exhibited high electrocatalytic activity for IMI, resulting in a fourfold increase in electrochemical signal. This prepared sensor offers high sensitivity for IMI with a LOD of 0.03 μ g mL⁻¹. Further, we constructed an antifouling electrochemical sensor for IMI determination in complex samples based on mesoporous silica film (MSF) coating electrochemically reduced graphene oxide/GCE (ErGO/MSF/GCE) (Figure 3c) [65]. This prepared sensor showed excellent performance for IMI determination due to the electrocatalytic activity of ErGO and the preconcentration ability of MSF towards IMI (Figure 3d). Mutharani et al. [22] synthesized cerium sulfide with gum arabic carbon flowers (Ce₂S₃/GACFs) through the hydrothermal method and employed it to monitor IMI (Figure 3b). The obtained Ce₂S₃/GACFs had a high surface area, which provided many electrocatalytic active sites for IMI reduction. This prepared sensor could detect IMI in a wide linear range of 0.05–1266 μ M with a LOD of 32 nM. Besides, other materials such as TiO₂ [66], bismuth film [67], graphene quantum dots/ionic liquid/multiwall carbon nanotubes (GQDs/IL/MWCNTs) [68] were also used to modify GCE and applied for IMI determination. The nanomaterials can improve the electrochemical response of IMI mainly

in two aspects: on the one hand, they can increase the active area of the electrode, and on the other hand, they can catalyze the reduction of IMI.

Table 2. Analytical performance of IMI detection based on direct electrochemical reduction.

Electrode Materials	Technique	Linear Range	LOD	Reference
GO/GCE	SWV ^a	10–200 μM	8.3 μM	[62]
GO/GCE	CV ^b	0.8–10 μM	0.36 μM	[69]
NGE-N/GCE ^e	DPV ^c	4–20.0 μM	0.55 μM	[70]
LIG ^f	SWV	Not given	384 nM	[63]
β -CDP/rGO/GCE ^g	DPV	0.05–15.0 μM , 20–150.0 μM	0.02 μM	[71]
E-rGO/ α -CD/GCE	LSV ^d	0.5–40.0 μM	20 nM	[64]
β -CD/MWCNT-MEA ^h	DPV	5.0–100.0 μM	0.629 μM	[72]
RPC@PANI/GCE ⁱ	CV	0.1–70 $\mu\text{g mL}^{-1}$	0.03 $\mu\text{g mL}^{-1}$	[10]
MSF/ErGO/GCE ^j	CV	1.0–50 $\mu\text{g mL}^{-1}$ 50–400 $\mu\text{g mL}^{-1}$	0.3 $\mu\text{g mL}^{-1}$	[65]
Ce ₂ S ₃ /GACFs/GCE ^k	DPV	0.391–274 μM	32 nM	[22]
GQDs/IL/MWCNTs/GCE ^l	DPV	0.03–12 μM	9 nM	[68]

^a SWV: Square-wave voltammetry; ^b CV: Cyclic voltammetry; ^c DPV: differential pulse voltammetry; ^d LSV: Linear Sweep Voltammetry. ^e NGE-N: vitamin B3 reduced nitrogen-doped graphene; ^f LIG: laser-induced graphene; ^g β -CDP: β -cyclodextrin polymer; ^h β -CD/MWCNT-MEA: β -cyclodextrin/multi-walled carbon nanotube (β -CD/MWCNT)-modified microelectrode array; ⁱ RPC@PANI: raffia derived porous carbon and polyaniline; ^j MSF/ErGO: mesoporous silica film/electrochemically reduced GO; ^k Ce₂S₃/GACFs: cerium sulfide with gum arabic carbon flowers; ^l GQDs/IL/MWCNTs: graphene quantum dots/ionic liquid/multiwall carbon nanotubes.

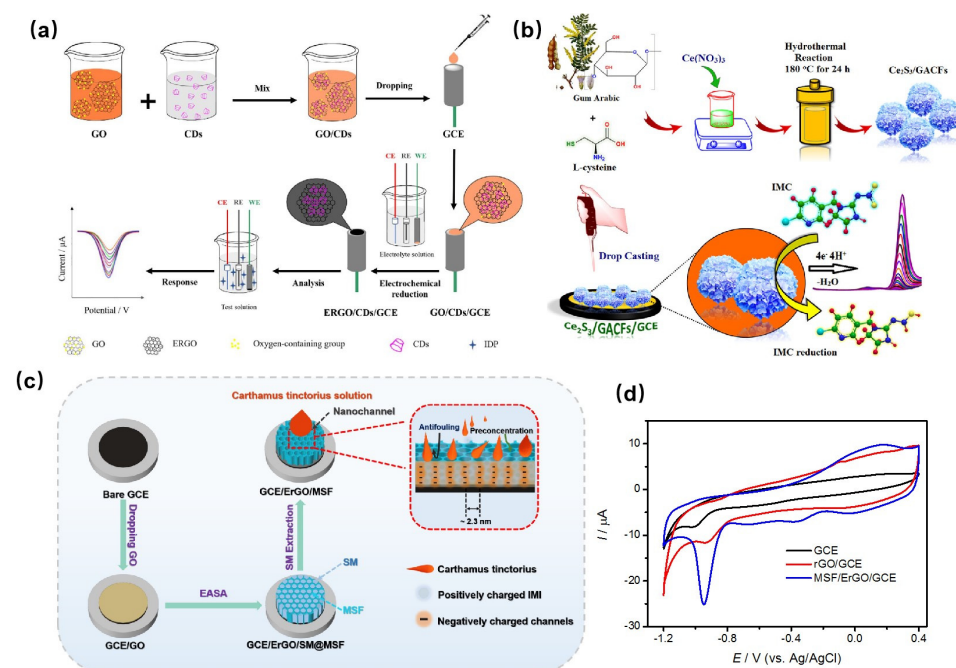


Figure 3. (a) Schematic procedure for the preparation of E-rGO/CDs/GCE. Reproduced from [64] with permission from Elsevier. (b) Schematic representation of the synthesis of Ce₂S₃/GACFs and its electrochemical detection of imidacloprid. Reproduced from [22] with permission from ACS. (c) Representation of the preparation of MSF/ErGO/GCE and its electrochemical detection of imidacloprid, and (d) CVs of different electrodes in 0.1 M HAc-NaAc buffer (pH 5.0) containing 20 $\mu\text{g mL}^{-1}$ IMI. Reproduced from [65] with permission from Elsevier.

3.2.2. Electrochemical Sensors Based on MIPs

Molecularly imprinted polymers (MIPs) are tailor-made synthetic materials with high-affinity binding sites for a specific target molecule [73]. MIPs are prepared by mixing a target molecule as a template with a cross-linking agent and an initiator. After polymerization, the

template is removed, leaving the hole exactly the same as the target molecule. The forming hole can rebind perfectly with the target molecule, allowing it to be specifically recognized and detected target molecule. Therefore, sensors based on MIPs have been designed and applied in various fields, such as environmental analysis [74], pharmaceutical analysis [75], nucleic acid assay [76], and food safety [77]. For instance, the Zhou group [78] prepared MIP on graphene oxide modified GCE by cyclic voltammetry, using IMI as the template and *o*-phenylenediamine (*o*-PD) as the functional monomer (Figure 4a). The imprinted electrode exhibited good selectivity toward IMI, detecting IMI in the concentration range of 0.75–70 μM with a LOD of 0.4 μM . The Wang group [79] synthesized MIP by chemical method, using *p*-vinylbenzoic acid (VBA) as functional monomer, IMI as template molecule, ethylene glycol dimethacrylate (EGDMA), and azobisisobutyronitrile (AIBN) as cross-linker and initiator. The prepared MIP was dropped on polished GCE and applied for IMI detection. This proposed sensor could detect IMI at 0.5–15 μM with a LOD of 0.1 μM . Moreover, it was successfully applied to detect IMI in brown rice samples. Tang et al. [80] prepared upconverting nanoparticles with a modified zeolite imidazolate framework and MIPs composite (MIPs/UCNPs@ZIF-8) for constructing an electrochemiluminescence (ECL) sensor. The obtained ECL sensor exhibited excellent performance for IMI detection in a concentration range of 0.1 ng L^{-1} to 1 mg L^{-1} with a LOD of 0.01 ng L^{-1} . Ma et al. [81] developed an ECL sensor for trace detection of IMI based on an ultrafine mixed-valence Ce-MOF (UMV-Ce-MOF) combined with MIP (Figure 4b,c). This proposed sensor could detect IMI with high sensitivity and selectivity.

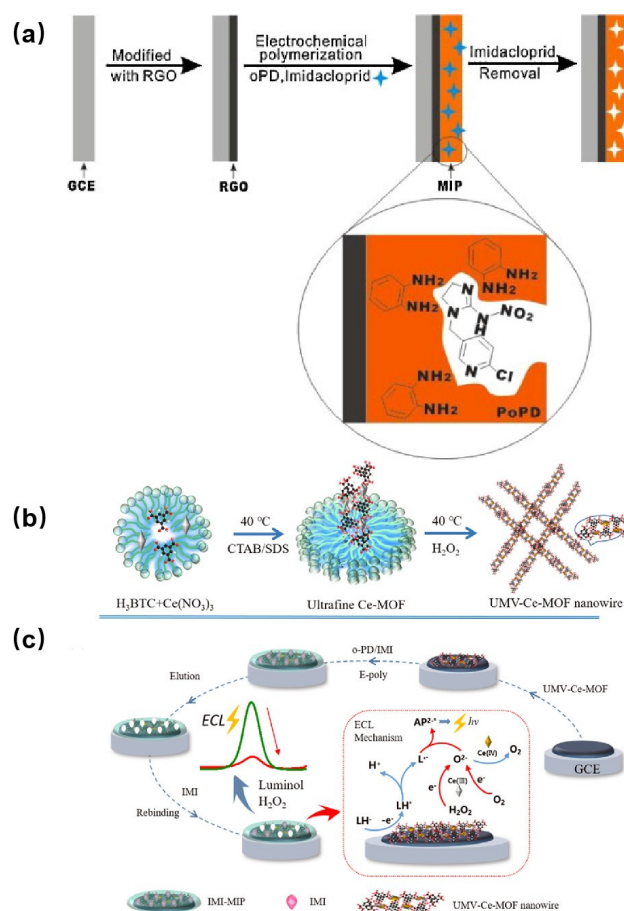


Figure 4. (a) The preparation of an imprinted PoPD-RGO electrode. Reproduced from [78] with permission from Elsevier. (b) Biomimetic synthesis of the UMV-Ce-MOF nanowires (c) and preparation of an imidacloprid sensor based on UMV-Ce-MOF nanowires. Reproduced from [81] with permission from ACS.

3.2.3. Electrochemical Sensor Based on Biometric Molecules

Except for MIP, some biometric recognition elements such as antibodies, enzymes, and aptamers have been used to improve the selectivity of sensors. Timur et al. [82] found an aptamer of IMI by the Systematic Evolution of Ligands by Exponential Enrichment (SELEX) process, and an aptasensor was constructed for IMI detection in a range of 0.1–50 ng mL⁻¹ with a LOD of 0.19 ng mL⁻¹. Pérez-Fernández et al. [83] reported a competitive immunosensor for IMI detection based on AuNPs-modified screen-printed carbon electrodes (AuNPs-SPCE). In this work, a monoclonal antibody to IMD (mAb-IMD) was immobilized on AuNPs-SPCE, and a competitive assay was performed between free IMI and IMI labeled with horseradish peroxidase (HRP). The electrochemical reduction signal of oxidized 3,3',5,5'-tetramethylbenzidine (TMB) was associated with IMI concentration, avoiding the use of secondary antibodies. This sensor exhibited excellent performance for IMI determination, with a satisfactory low LOD, high selectivity, and stability. Furthermore, this sensor was successfully applied in IMI analysis on a real sample, and the reliability was also validated by HPLC-MS/MS. Table 3 concludes the analytical performance of electrochemical IMI detection based on recognition elements such as MIP, antibodies, and aptamers.

Table 3. Analytical performance of the electrochemical method for IMI detection based on recognition molecules.

Electrode Materials	Recognition Element	Technique	Linear Range	LOD	Reference
PoPD-RGO/GCE ^a	MIP	LSV	0.75–70 μM	0.4 μM	[78]
GN/MIPs/GCE ^b	MIP	LSV	0.5–15 μM	0.1 μM	[79]
GCE/TiO ₂ NPs/IMD imprinted poly(levodopa)	MIP	SWV	2.0–400 μM	0.3 μM	[84]
UMV-Ce-MOF ^c	MIP	ECL	2–120 nM	0.34 nM	[81]
MIPs/UCNPs@ZIF-8/GCE ^d	MIP	ECL	0.1 ng mL ⁻¹ –mg mL ⁻¹	0.01 ng mL ⁻¹	[80]
Gold electrode	aptamer	EIS ^f	0.1–50 ng mL ⁻¹	0.19 ng mL ⁻¹	[82]
AuNP-SPCE ^e	antibody	chronoamperometry	50–10,000 pM	22 pM	[83]
SPCE	antibody	chronoamperometry	50–10,000 pM	24 pM	[85]

^a PoPD-RGO: imprinted poly(o-phenylenediamine) (PoPD) membranes at reduced graphene oxide (RGO); ^b GN: graphene; ^c UMV-Ce-MOF: ultrafine mixed-valence Ce-MOF; ^d UCNPs@ZIF-8: upconverting nanoparticle functional zeolite imidazolate framework; ^e AuNP-SPCE: gold nanoparticle-modified screen-printed carbon electrodes (SPCE); ^f EIS: electrochemical impedance spectroscopy.

3.2.4. Ratiometric Electrochemical Sensor

The classical electrochemical sensor contains only a single electrochemical signal of the target molecule, and its reproducibility is easily influenced by electrode properties or the complex detection system. To overcome this limitation, ratiometric electrochemical sensors involving the simultaneous measurement of two electrochemical signals at different potentials have been developed. By introducing a built-in correction for the analyte's signal, the ratio electrochemical sensor greatly improves the reproducibility and reliability of electrochemical detection. So far, ratio electrochemical sensors have been used to detect metal ions, nucleic acids, proteins, biological small molecules, etc. [86,87]. The researchers also applied the ratio sensing strategy for IMI detection. The Kan group [88] constructed a ratio electrochemical sensor by electropolymerization of thionine and β-CD composite on GCE for IMI determination, in which thionine as an internal reference element provides a built-in correction. The current ratio of IMI and thionine was employed as the signal for IMI detection, and it exhibited a good linear relationship in the concentration range of 0.04–10 μM. The Zou group [89] prepared a ratio electrochemical sensor coupled with a MIP strategy for IMI detection, in which 6-(Ferrocenyl)hexanethiol (FcHT) is used as an

inner reference and MIP as a molecular recognition receptor (Figure 5). The combination of ratiometric strategy and MIP enhances the sensitivity and selectivity of the sensor.

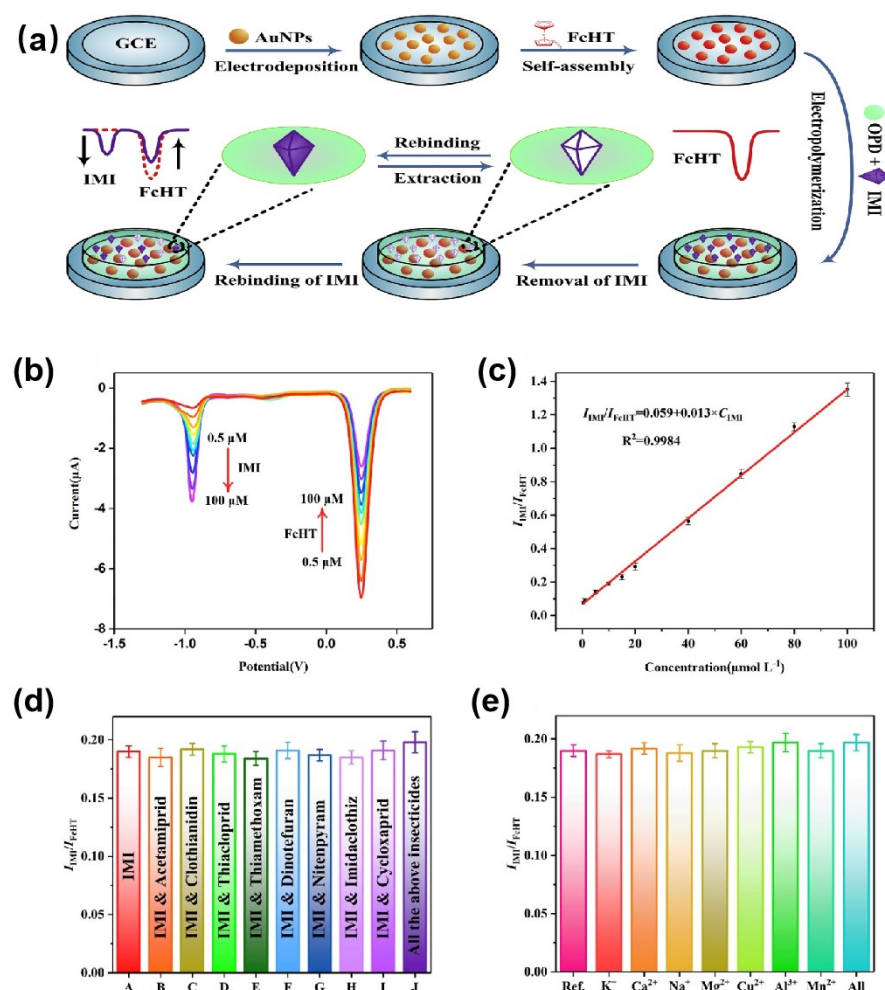


Figure 5. (a) Schematic diagram of the fabrication process of the MIP/FcHT/AuNPs electrode. The performance of the proposed sensor: (b) DPV responses and (c) calibration curve of the MIP/FcHT/AuNPs electrode in PBS after incubation with different concentrations of IMI. Selectivity of the MIP/FcHT/AuNPs electrode in the presence of (d) IMI analogs or (e) metal ions. Reproduced from [89] with permission from Elsevier.

To sum up, researchers have developed a variety of electrochemical sensing strategies based on nanomaterials for IMI detection. On the one hand, designing and synthesizing nanomaterials with controlled morphology or preparing hybrid materials to further improve the electrocatalytic reduction of IMI is highly necessary. On the other hand, combining the advantages of easy miniaturization of electrochemical sensors with specific recognition elements, the establishment of hand-held electrochemical sensing devices with high selectivity and sensitivity has great prospects.

3.3. Optical Sensors

Over the past decades, researchers have devoted intensive efforts to developing various optical sensors due to their advantages, including simplicity, ultra-sensitivity, and high selectivity. The principle of an optical sensor is based on the shift of the characteristic signal caused by the interaction of the analyte with the substrate or with other optical molecules. With the development of nanotechnology, many optical detection platforms have been born. According to the different detection signals, multiple optical sensors, including

fluorescence, colorimetry, surface plasmon resonance (SPR), and surface enhanced Raman spectroscopy (SERS), have been applied to detect IMI (Table 4).

3.3.1. Fluorescent Method

Recently, with the significant development of optical nanomaterials, fluorescence sensing has dramatically benefited from various luminescent nanoparticles. For instance, Tian et al. [90] developed two kinds of lateral flow immunoassay (LFIA) for IMI determination based on time-resolved fluorescent nanobeads and colloidal gold, respectively. The proposed LFIA achieved high accuracy and a low LOD for IMI analysis. Guo et al. [12] established a competitive fluorescence resonance energy transfer (FRET) immunoassay for IMI detection (Figure 6a). FRET occurred through the specific immunoreaction between antigen/GO and mAb/up-converting nanoparticles, (UCNPs). The fluorescence intensity of UCNPs was weakened by GO, and the fluorescent recovery of UCNPs is associated with IMI concentration through the competitive mechanism. This sensor showed a wide range of 0.08–50 ng/mL for IMI in the presence of other interferences. Li et al. [91] proposed a fluorescence-based immunoassay (FIA) for IMI, in which multiple strategies were involved (Figure 6b). In details, firstly, gold nanoclusters (AuNCs) were loaded on cobalt oxyhydroxide (CoOOH) nanoflakes by electrostatic interaction, in which the fluorescence intensity of AuNCs was suppressed by CoOOH by FRET. Secondly, the fluorescence of AuNCs recovered due to the decomposition of CoOOH nanoflakes triggered by ascorbic acid (AA), which was produced through enzyme-induced L-ascorbic acid-2-phosphate (AAP) hydrolysis. Clearly, the fluorescence response of AuNCs was related to the ALP activity labeled on the antibody. Thirdly, in the presence of IMI, the amount of labeled ALP decreased due to competitive immunoreaction, resulting in a decrease in the fluorescence intensity of AuNCs. The fluorescence change of AuNCs was related to the concentration of IMI, so the quantitative detection of IMI could be realized (Figure 6c,d). This FIA protocol was 60 times more sensitive than that of a conventional enzyme-linked immunosorbent assay (ELISA), and a low LOD of 1.3 ng mL⁻¹ was obtained.

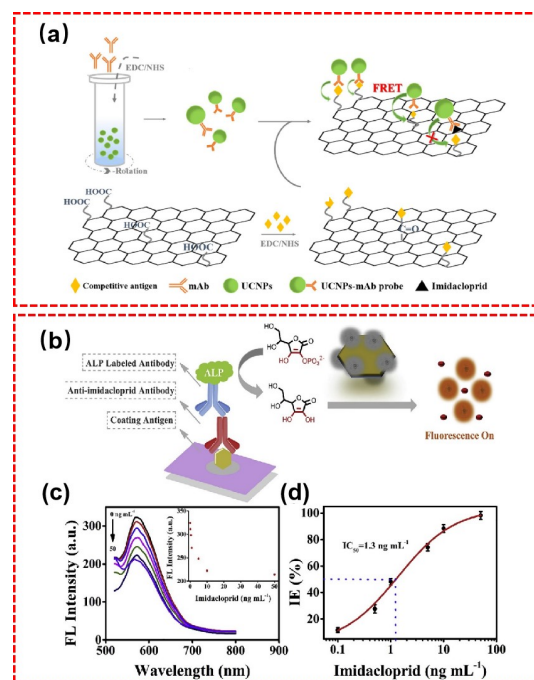


Figure 6. (a) Schematic of the FRET immunoassay between UCNPs and GO for one-step detection of imidacloprid residue. Reproduced from [12] with permission from Elsevier. (b) Schematic representation of FIA. (c) The FL spectra of the FIA toward imidacloprid standards with various concentrations (0, 0.1, 0.5, 1.0, 5.0, 10, and 50 ng mL⁻¹). (d) The linear plot of IE (%) versus the concentration of imidacloprid. Reproduced from [91] with permission from Elsevier.

3.3.2. Colorimetric and Surface Plasmon Resonance (SPR) Sensors

A colorimetric sensor has the merits of visualization, simplicity, low cost, and being a powerful tool for high-throughput analysis. In recent years, various noble metal nanoparticles, such as AuNPs and AgNPs, have been applied for the construction of colorimetric sensors owing to their strong localized surface plasmon resonance (LSPR) effect. Further, plasmonic colorimetric sensors based on metal nanoparticles have been applied to detect various analytes, including metal ions, pesticides, proteins, DNA, pathogens, and so on [92–96]. For example, Tian et al. [97] developed a colorimetric sensor for IMI based on the induced-aggregation property of prperidine-calix [4] arene modified AuNPs (PPC-AuNPs), and this sensor could detect IMI with high sensitivity and a LOD of 0.25 μM . Zhao et al. [98] proposed colorimetric sensors for different pesticides based on their inhibition of acetylcholinesterase (AChE) using diverse AuNPs (Figure 7a), and this method could successfully distinguish eight pesticides by linear discriminant analysis (LDA) (Figure 7b). More importantly, a portable device was constructed by combing this method with a smartphone (Figure 7c). Wang et al. [99] designed a label-free SPR sensing platform with a multichannel spectral imaging system, which enabled high-throughput quantified detection of IMI and fipronil (Figure 8). More importantly, this custom-made integrated system could allow on-site detection, which was an improvement over chromatographic methods.

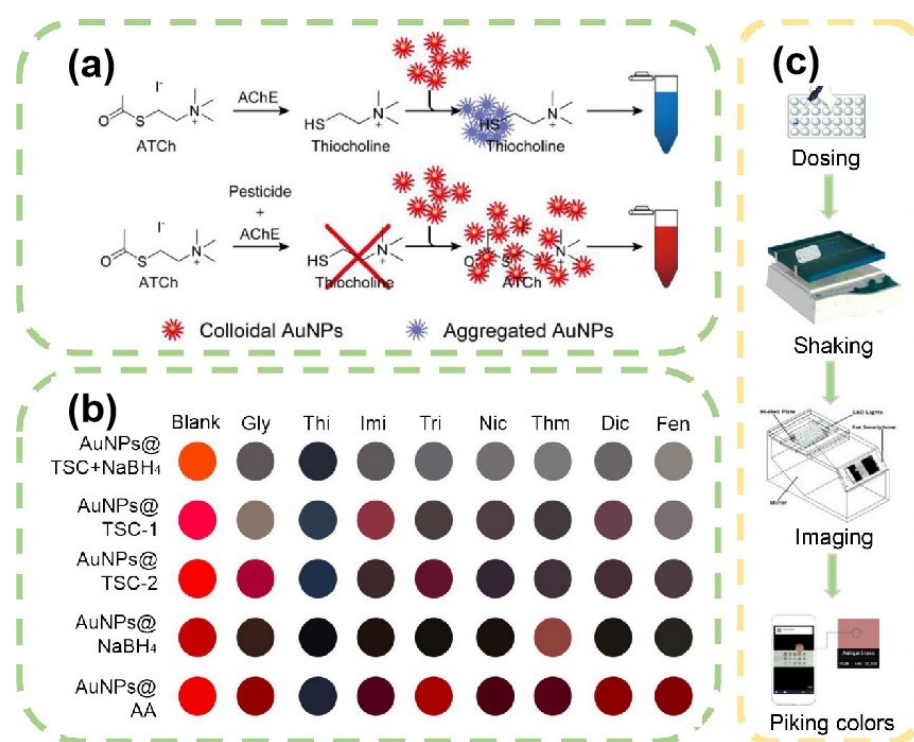


Figure 7. The principle and working process of the AuNP-based colorimetric sensor array for distinguishing multiple pesticides. (a) The mechanism of distinguishing multiple pesticides by combining AChE and AuNP-based colorimetric sensor arrays. (b) The schematic diagram of the colorimetric sensor-array result. (c) The main procedures of the working process are dosing, shaking, imaging, and picking colors. Reproduced from [98] with permission from Elsevier.

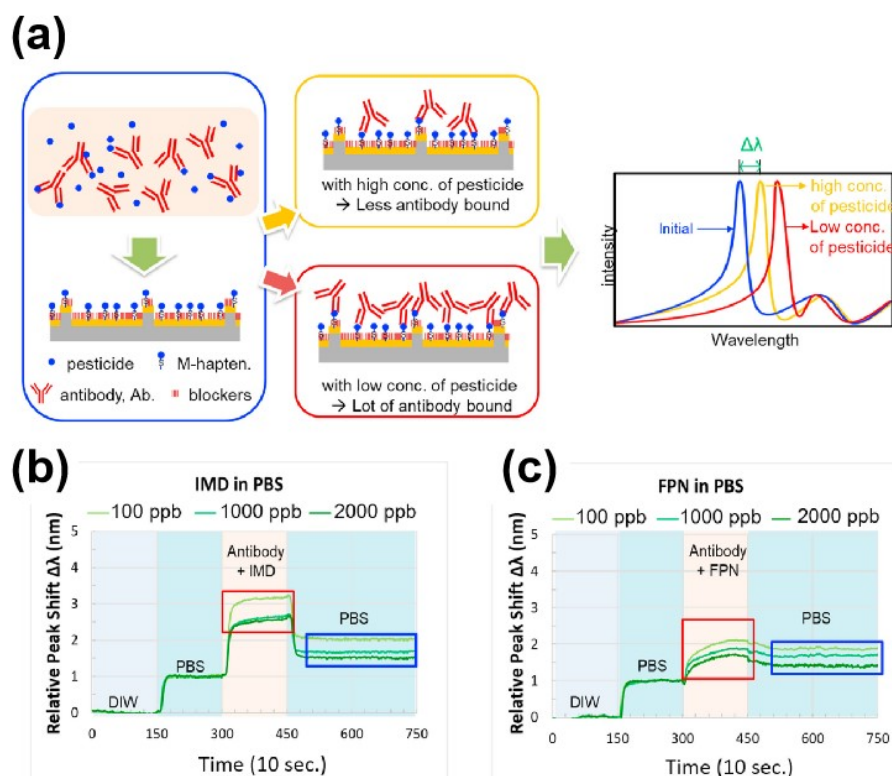


Figure 8. (a) Illustration of the competitive binding immunoassay and the induced signal difference in the SPR peak shift. The blocker used here is 2-mercaptoethanol. Kinetic SPR curves of (b) imidacloprid and (c) fipronil; abbreviations: SPR, surface plasmonic resonance; IMD, imidacloprid; FPN, fipronil; DIW, deionized water; PBS, phosphate-buffered saline. Reproduced from [99] with permission from Elsevier.

3.3.3. Surface-Enhanced Raman Spectroscopy

The Surface Enhanced Raman Scattering (SERS) technique has received much attention in the field of analysis due to its non-invasive and unique fingerprint characteristics. In particular, the Raman signal can be enhanced with the use of nanomaterials with plasmonic properties, greatly improving the sensitivity of detection. For example, the O’Riordan group [100] proposed a SERS sensor for two neonicotinoids, including clothianidin and IMI, using Ag nanoparticles coated Polyvinylidene fluoride (PVDF) substrates. The developed SERS can sense 1 ng/mL IMI with a LOD of 4 nM. More importantly, in this work, the authors provide the detailed vibrational characteristics of IMI in combination with first-principle simulations. Sun et al. [101] developed a SERS sensor for IMI with a competitive immune strategy (Figure 9). In this work, a Raman tag containing $C\equiv N$ ($1800\text{--}2800\text{ cm}^{-1}$) bond was anchored on an AuNR@Ag nanocuboid to resist the optical interference from the fingerprint region ($<1800\text{ cm}^{-1}$) and an antibody was used to specifically identify IMI. In addition, the Fe_3O_4 nanoparticles were used to achieve magnetic separation and improve the SERS intensity. This SERS immunosensor can detect IMI at 10–40 nM with high selectivity. Sheng et al. [24] developed a SERS-based lateral flow assay (SERS-LFA) test strip for detection of IMI, chlorothalonil (CHL), and oxyfluorfen (OXY) simultaneously with a competitive immune strategy. In this work, the prepared silver-core, gold-shell (Ag@Au) nanoprobe was used to fix the SERS signal molecule 4-nitrothiophenol (4-NTP), connect antibodies, and enhance the SERS signal. This SERS-LFA test strip gains reliable results with rapid response, high sensitivity, low LOD, and low cost. The detection sensitivity was closely related to the type of SERS base materials.

Table 4. Analytical performance of IMI detection based on optical methods.

Methods	Materials	Linear Range	LOD	Reference
colorimetry	PPC-Au NPs ¹	0.05–1000 μM	5.0 μM	[97]
colorimetry	I-IL-Au NPs ²	Not given	0.5 μM	[102]
SPR immunoassay	Nanoplasmonic chips	Not given	11.103 ppb	[99]
SPR immunoassay	plasmonic biochip	Not given	0.2 ng mL^{-1}	[103]
fluorescence	CoOOH-AuNCs	0.1 ng mL^{-1} –50 ng mL^{-1}	0.1 ng mL^{-1}	[91]
fluorescence	colloidal gold	0.028 ng mL^{-1} –0.5 ng mL^{-1}	0.01 ng mL^{-1}	[90]
fluorescence	GO-UCNPs ³	0.08 ng mL^{-1} –50 ng mL^{-1}	0.08 ng mL^{-1}	[12]
SERS immunosensor	Fe_3O_4 -AuNR@Ag	10–400 nM	9.58 nM	[101]
LSPR immunosensor	Y-shaped gold NPs	Not given	1.0 ng mL^{-1}	[104]
ratiometric fluorescence	MIFP-SiCQDs@CdTe QDs ⁴	5 ng mL^{-1} –0.5 $\mu\text{g mL}^{-1}$	3.55 ng mL^{-1}	[105]

¹ PPC-Au NPs: piperidine-calix [4] arene modified gold nanoparticles; ² I-IL-Au NPs: onimidazole ionic liquid (IL) modified gold nanoparticles; ³ GO-UCNPs: graphene oxide (GO) and up-converting nanoparticles (UCNPs); ⁴ MIFP-SiCQDs@CdTe QDs: molecularly imprinted multilevel mesoporous silica.

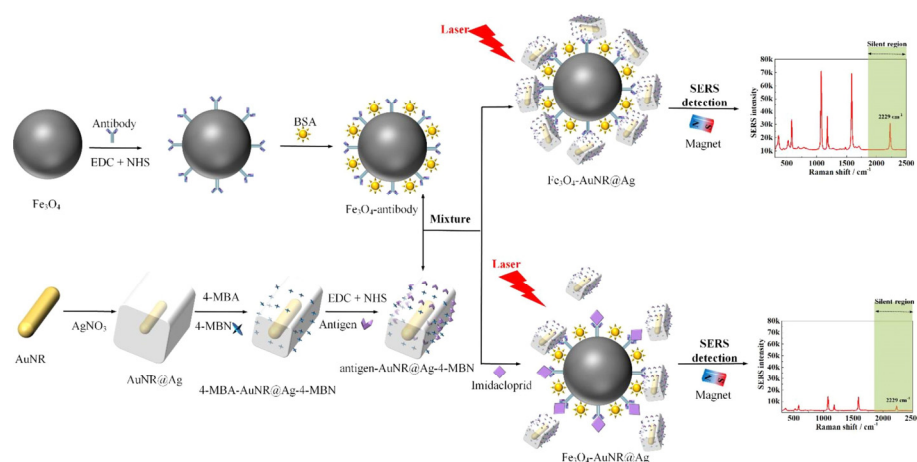


Figure 9. Scheme showing the competitive immunoassay detection procedures (4-MBN: 4-mercaptobenzonitrile; 4-MBA: 4-mercaptobenzoic acid; BSA: bovine serum albumin; EDC: (3-dimethylaminopropyl)-3-ethylcarbodiimide hydrochloride; NHS: N-hydroxysuccinimide). Reproduced from [101] with permission from Elsevier.

4. Conclusions and Outlook

This review summarized the impressive recent works on sensors for IMI using various nanomaterials, and the functions of nanomaterials in different analytical techniques (chromatographic, electrochemical, and optical) were described. From the comprehensive analysis results displayed in Tables 1–3, it can be seen that nanomaterials play significant roles in designing novel sensors, and the analytical performance of sensors is greatly improved with the incorporation of nanomaterials. For sample preparation, various pre-treatment methods have been designed to remove matrix interference and pre-enrich the targets based on functional nanomaterials. Subsequently, multiple chromatographic techniques were used for the accurate detection of IMI and its metabolites. In electrochemical and optical methods, nanomaterials are mainly used for immobilizing specific molecules and amplifying signals. Moreover, the selective detection of IMI has been realized with the help of MIP and biometric molecules.

Although researchers have developed a variety of highly sensitive sensors for IMI detection, these sensing systems still face several problems and challenges. Hence, we suggest that further research perspectives in this field be taken into account: (1) decrease the testing cost of sensors; (2) continuous real-time monitoring of IMI during crop growth; (3) portable microdevices for field detection; (4) long-term stability of sensors in complex

real samples. By considering the abovementioned problems, the development of various sensors should be combined with other advanced technologies, such as the microfluidic technique, to give full play to the advantages of portability and miniaturization of microfluidic devices. On the other hand, antifouling sensing platforms need to be established to maintain their stability on complex substrates.

Author Contributions: Writing—original draft preparation, S.C., Y.W. and X.L.; writing—review and editing, L.D.; supervision, L.D.; funding acquisition, L.D. All authors have read and agreed to the published version of the manuscript.

Funding: This research was funded by the National Natural Science Foundation of China (51802118) and the Natural Science Foundation of Shandong Province (2018GSF118166).

Institutional Review Board Statement: Not applicable.

Informed Consent Statement: Not applicable.

Data Availability Statement: Not applicable.

Conflicts of Interest: The authors declare no conflict of interest.

References

1. Jeschke, P.; Nauen, R. Neonicotinoids—From zero to hero in insecticide chemistry. *Pest. Manag. Sci.* **2008**, *64*, 1084–1098. [[CrossRef](#)] [[PubMed](#)]
2. Li, Q.; Kong, X.; Xiao, Z.; Zhang, L.; Wang, F.; Zhang, H.; Li, Y.; Wang, Y. Structural determinants of imidacloprid-based nicotinic acetylcholine receptor inhibitors identified using 3D-QSAR, docking and molecular dynamics. *J. Mol. Model.* **2012**, *18*, 2279–2289. [[CrossRef](#)] [[PubMed](#)]
3. Sriapha, C.; Trakulsrichai, S.; Intaraprasong, P.; Wongvisawakorn, S.; Tongpoo, A.; Schimmel, J.; Wananukul, W. Imidacloprid poisoning case series: Potential for liver injury. *Clin. Toxicol.* **2020**, *58*, 136–138. [[CrossRef](#)] [[PubMed](#)]
4. Millot, F.; Decors, A.; Mastain, O.; Quintaine, T.; Berny, P.; Vey, D.; Lasseur, R.; Bro, E. Field evidence of bird poisonings by imidacloprid-treated seeds: A review of incidents reported by the French SAGIR network from 1995 to 2014. *Environ. Sci. Pollut. Res.* **2017**, *24*, 5469–5485. [[CrossRef](#)]
5. Wan, Y.; Han, Q.; Wang, Y.; He, Z. Five degradates of imidacloprid in source water, treated water, and tap water in Wuhan, central China. *Sci. Total Environ.* **2020**, *741*, 140227. [[CrossRef](#)]
6. European Food Safety Authority. Neonicotinoids: Risk to Bees Confirmed. 2018. Available online: <https://www.efsa.europa.eu/en/press/news/180228> (accessed on 1 June 2022).
7. Yang, B.; Ma, W.; Wang, S.; Shi, L.; Li, X.; Ma, Z.; Zhang, Q.; Li, H. Determination of eight neonicotinoid insecticides in Chinese cabbage using a modified QuEChERS method combined with ultra performance liquid chromatography-tandem mass spectrometry. *Food Chem.* **2022**, *387*, 132935. [[CrossRef](#)]
8. Wang, Y.; Fu, Y.; Wang, Y.; Lu, Q.; Ruan, H.; Luo, J.; Yang, M. A comprehensive review on the pretreatment and detection methods of neonicotinoid insecticides in food and environmental samples. *Food Chem. X* **2022**, *15*, 100375. [[CrossRef](#)]
9. Liu, L.; Guo, J.; Liu, X.; Wang, A.; Yu, X.; Ding, L. Photoelectrochemical Clothianidin Detection Based on a WO₃/CdS Heterostructure Coated with a Molecularly Imprinted Thin Film. *Anal. Sens.* **2022**, *2*, e202200029. [[CrossRef](#)]
10. Liu, L.; Guo, J.; Ding, L. Polyaniline Nanowire Arrays Deposited on Porous Carbon Derived from *Raffia* for Electrochemical Detection of Imidacloprid. *Electroanalysis* **2021**, *33*, 2048–2052. [[CrossRef](#)]
11. Guo, J.-W.; Yang, Z.-W.; Liu, X.-L.; Zhang, L.-W.; Guo, W.-B.; Zhang, J.; Ding, L.-H. 2D Co metal-organic framework nanosheet as an oxidase-like nanozyme for sensitive biomolecule monitoring. *Rare Met.* **2023**, *42*, 797–805. [[CrossRef](#)]
12. Guo, Y.; Zou, R.; Si, F.; Liang, W.; Zhang, T.; Chang, Y.; Qiao, X.; Zhao, J. A sensitive immunoassay based on fluorescence resonance energy transfer from up-converting nanoparticles and graphene oxide for one-step detection of imidacloprid. *Food Chem.* **2021**, *335*, 127609. [[CrossRef](#)]
13. Gao, L.; He, C. Application of nanomaterials decorated with cyclodextrins as sensing elements for environment analysis. *Environ. Sci. Pollut. Res.* **2021**, *28*, 59499–59518. [[CrossRef](#)] [[PubMed](#)]
14. Kumar, S.; Wang, Z.; Zhang, W.; Liu, X.; Li, M.; Li, G.; Zhang, B.; Singh, R. Optically Active Nanomaterials and Its Biosensing Applications—A Review. *Biosensors* **2023**, *13*, 85. [[CrossRef](#)] [[PubMed](#)]
15. Xue, X.-y.; Cheng, R.; Shi, L.; Ma, Z.; Zheng, X. Nanomaterials for water pollution monitoring and remediation. *Environ. Chem. Lett.* **2017**, *15*, 23–27. [[CrossRef](#)]
16. Ahmadi, M.; Elmongy, H.; Madrakian, T.; Abdel-Rehim, M. Nanomaterials as sorbents for sample preparation in bioanalysis: A review. *Anal. Chim. Acta* **2017**, *958*, 1–21. [[CrossRef](#)] [[PubMed](#)]
17. Ding, L.; Yan, J.; Zhao, Z.; Li, D. Synthesis of NiGa₂O₄ nanosheets for non-enzymatic glucose electrochemical sensor. *Sens. Actuators B Chem.* **2019**, *296*, 126705. [[CrossRef](#)]

18. Ding, L.; Ma, C.; Li, L.; Zhang, L.; Yu, J. A photoelectrochemical sensor for hydrogen sulfide in cancer cells based on the covalently and in situ grafting of CdS nanoparticles onto TiO₂ nanotubes. *J. Electroanal. Chem.* **2016**, *783*, 176–181. [[CrossRef](#)]
19. An, H.; Li, M.; Ga, J.; Zhang, Z.; Ma, S.; Chen, Y. Incorporation of biomolecules in Metal-Organic Frameworks for advanced applications. *Coord. Chem. Rev.* **2019**, *384*, 90–106. [[CrossRef](#)]
20. Bilal, M.; Asgher, M.; Cheng, H.; Yan, Y.; Iqbal, H.M.N. Multi-point enzyme immobilization, surface chemistry, and novel platforms: A paradigm shift in biocatalyst design. *Crit. Rev. Biotechnol.* **2019**, *39*, 202–219. [[CrossRef](#)]
21. Ding, L.; Zhang, L.; Yang, H.; Liu, H.; Ge, S.; Yu, J. Electrochemical biosensor for p53 gene based on HRP-mimicking DNAzyme-catalyzed deposition of polyaniline coupled with hybridization chain reaction. *Sens. Actuators B Chem.* **2018**, *268*, 210–216. [[CrossRef](#)]
22. Mutharani, B.; Keerthi, M.; Chen, S.-M.; Ranganathan, P.; Chen, T.-W.; Lee, S.-Y.; Chang, W.-H. One-Pot Sustainable Synthesis of Ce₂S₃/Gum Arabic Carbon Flower Nanocomposites for the Detection of Insecticide Imidacloprid. *ACS Appl. Mater. Interfaces* **2020**, *12*, 4980–4988. [[CrossRef](#)]
23. Mou, B.; Zuo, C.; Chen, L.; Xie, H.; Zhang, W.; Wang, Q.; Wen, L.; Gan, N. On-site Simultaneous Determination of Neonicotinoids, Carbamates, and Phenyl Pyrazole Insecticides in Vegetables by QuEChERS Extraction on Nitrogen and Sulfur co-doped Carbon Dots and Portable Mass Spectrometry. *J. Chromatogr. A* **2023**, *1689*, 463744. [[CrossRef](#)]
24. Sheng, E.; Lu, Y.; Xiao, Y.; Li, Z.; Wang, H.; Dai, Z. Simultaneous and ultrasensitive detection of three pesticides using a surface-enhanced Raman scattering-based lateral flow assay test strip. *Biosens. Bioelectron.* **2021**, *181*, 113149. [[CrossRef](#)] [[PubMed](#)]
25. Thompson, D.A.; Lehmler, H.-J.; Kolpin, D.W.; Hladik, M.L.; Vargo, J.D.; Schilling, K.E.; LeFevre, G.H.; Peeples, T.L.; Poch, M.C.; LaDuca, L.E.; et al. A critical review on the potential impacts of neonicotinoid insecticide use: Current knowledge of environmental fate, toxicity, and implications for human health. *Environ. Sci. Process. Impacts* **2020**, *22*, 1315–1346. [[CrossRef](#)] [[PubMed](#)]
26. Loser, D.; Grillberger, K.; Hinojosa, M.G.; Blum, J.; Haufe, Y.; Danker, T.; Johansson, Y.; Möller, C.; Nicke, A.; Bennekou, S.H.; et al. Acute effects of the imidacloprid metabolite desnitro-imidacloprid on human nACh receptors relevant for neuronal signaling. *Arch. Toxicol.* **2021**, *95*, 3695–3716. [[CrossRef](#)] [[PubMed](#)]
27. Brunet, J.-L.; Maresca, M.; Fantini, J.; Belzunces, L.P. Human intestinal absorption of imidacloprid with Caco-2 cells as enterocyte model. *Toxicol. Appl. Pharmacol.* **2004**, *194*, 1–9. [[CrossRef](#)]
28. Zhang, Q.; Wang, X.; Rao, Q.; Chen, S.; Song, W. Imidacloprid dissipation, metabolism and accumulation in *Agaricus bisporus* fruits, casing soil and compost and dietary risk assessment. *Chemosphere* **2020**, *254*, 126837. [[CrossRef](#)]
29. Suchail, S.; Guez, D.; Belzunces, L.P. Discrepancy between acute and chronic toxicity induced by imidacloprid and its metabolites in *Apis mellifera*. *Environ. Toxicol. Chem.* **2001**, *20*, 2482–2486. [[CrossRef](#)]
30. Eng, M.L.; Hao, C.; Watts, C.; Sun, F.; Morrissey, C.A. Characterizing imidacloprid and metabolites in songbird blood with applications for diagnosing field exposures. *Sci. Total Environ.* **2021**, *760*, 143409. [[CrossRef](#)]
31. Jiao, X.; Li, Z.; He, J.; Wang, C. Enhanced photodegradation of applied dithianon fungicides on plant leaves by dissolved substances in atmosphere under simulated sunlight. *Chemosphere* **2020**, *254*, 126807. [[CrossRef](#)]
32. Codling, G.; Al Naggar, Y.; Giesy, J.P.; Robertson, A.J. Concentrations of neonicotinoid insecticides in honey, pollen and honey bees (*Apis mellifera* L.) in central Saskatchewan, Canada. *Chemosphere* **2016**, *144*, 2321–2328. [[CrossRef](#)] [[PubMed](#)]
33. Wu, C.; Dong, F.; Mei, X.; Ning, J.; She, D. Distribution, Dissipation, and Metabolism of Neonicotinoid Insecticides in the Cotton Ecosystem under Foliar Spray and Root Irrigation. *J. Agric. Food Chem.* **2019**, *67*, 12374–12381. [[CrossRef](#)] [[PubMed](#)]
34. Song, S.; Zhang, C.; Chen, Z.; He, F.; Wei, J.; Tan, H.; Li, X. Simultaneous determination of neonicotinoid insecticides and insect growth regulators residues in honey using LC–MS/MS with anion exchanger-disposable pipette extraction. *J. Chromatogr. A* **2018**, *1557*, 51–61. [[CrossRef](#)] [[PubMed](#)]
35. Sánchez-Hernández, L.; Hernández-Domínguez, D.; Bernal, J.; Neusüß, C.; Martín, M.T.; Bernal, J.L. Capillary electrophoresis–mass spectrometry as a new approach to analyze neonicotinoid insecticides. *J. Chromatogr. A* **2014**, *1359*, 317–324. [[CrossRef](#)] [[PubMed](#)]
36. Li, S.; Yu, P.; Zhou, C.; Tong, L.; Li, D.; Yu, Z.; Zhao, Y. Analysis of pesticide residues in commercially available chenpi using a modified QuEChERS method and GC-MS/MS determination. *J. Pharm. Anal.* **2020**, *10*, 60–69. [[CrossRef](#)]
37. Li, S.; Xu, H.; Sui, Y.; Mei, X.; Shi, J.; Cai, S.; Xiong, T.; Carrillo, C.; Castagnini, J.M.; Zhu, Z.; et al. Comparing the LC-MS Phenolic Acids Profiles of Seven Different Varieties of Brown Rice (*Oryza sativa* L.). *Foods* **2022**, *11*, 1552. [[CrossRef](#)]
38. Ingle, R.G.; Zeng, S.; Jiang, H.; Fang, W.-J. Current developments of bioanalytical sample preparation techniques in pharmaceuticals. *J. Pharm. Anal.* **2022**, *12*, 517–529. [[CrossRef](#)] [[PubMed](#)]
39. Zhao, W.-H.; Shi, Y.-P. A porous boron nitride nanorods-based QuEChERS analysis method for detection of five neonicotinoid pesticide residues in goji berries. *J. Chromatogr. A* **2022**, *1670*, 462968. [[CrossRef](#)]
40. Song, Z.; Li, J.; Lu, W.; Li, B.; Yang, G.; Bi, Y.; Arabi, M.; Wang, X.; Ma, J.; Chen, L. Molecularly imprinted polymers based materials and their applications in chromatographic and electrophoretic separations. *TrAC Trends Anal. Chem.* **2022**, *146*, 116504. [[CrossRef](#)]
41. Tao, X.-y.; Zhang, Y.; Zhou, Y.; Liu, Z.-f.; Feng, X.-s. Nicotine in Complex Samples: Recent Updates on the Pretreatment and Analysis Method. *Crit. Rev. Anal. Chem.* **2021**. [[CrossRef](#)]
42. Abdel-Ghany, M.F.; Hussein, L.A.; El Azab, N.F.; El-Khatib, A.H.; Linscheid, M.W. Simultaneous determination of eight neonicotinoid insecticide residues and two primary metabolites in cucumbers and soil by liquid chromatography-tandem mass spectrometry coupled with QuEChERS. *J. Chromatogr. B* **2016**, *1031*, 15–28. [[CrossRef](#)] [[PubMed](#)]

43. Zhang, B.-T.; Zheng, X.; Li, H.-F.; Lin, J.-M. Application of carbon-based nanomaterials in sample preparation: A review. *Anal. Chim. Acta* **2013**, *784*, 1–17. [[CrossRef](#)] [[PubMed](#)]
44. Che, D.; Cheng, J.; Ji, Z.; Zhang, S.; Li, G.; Sun, Z.; You, J. Recent advances and applications of polydopamine-derived adsorbents for sample pretreatment. *TrAC Trends Anal. Chem.* **2017**, *97*, 1–14. [[CrossRef](#)]
45. Zhang, H.; Xiong, P.; Li, G.; Liao, C.; Jiang, G. Applications of multifunctional zirconium-based metal-organic frameworks in analytical chemistry: Overview and perspectives. *TrAC Trends Anal. Chem.* **2020**, *131*, 116015. [[CrossRef](#)]
46. Selahle, S.K.; Mpupa, A.; Nomngongo, P.N. Combination of zeolitic imidazolate framework-67 and magnetic porous porphyrin organic polymer for preconcentration of neonicotinoid insecticides in river water. *J. Chromatogr. A* **2022**, *1661*, 462685. [[CrossRef](#)]
47. Wang, X.-H.; Li, W.; Jiang, H.-X.; Chen, Y.; Gao, R.-Z.; Tang, A.-N.; Kong, D.-M. Heteropore covalent organic framework-based composite membrane prepared by in situ growth on non-woven fabric for sample pretreatment of food non-targeted analysis. *Microchim. Acta* **2021**, *188*, 235. [[CrossRef](#)]
48. Wang, R.; Jiang, H.-X.; Jia, H.; Li, W.; Chen, Y.; Tang, A.-N.; Shao, B.; Kong, D.-M. Easily operated COF-based monolithic sponges as matrix clean-up materials for non-targeted analysis of chemical hazards in oil-rich foods. *Talanta* **2023**, *255*, 124250. [[CrossRef](#)]
49. Zhang, Y.; Li, G.; Wu, D.; Li, X.; Yu, Y.; Luo, P.; Chen, J.; Dai, C.; Wu, Y. Recent advances in emerging nanomaterials based food sample pretreatment methods for food safety screening. *TrAC Trends Anal. Chem.* **2019**, *121*, 115669. [[CrossRef](#)]
50. Xu, Y.; Li, X.; Zhang, W.; Jiang, H.; Pu, Y.; Cao, J.; Jiang, W. Zirconium(IV)-based metal-organic framework for determination of imidacloprid and thiamethoxam pesticides from fruits by UPLC-MS/MS. *Food Chem.* **2020**, *344*, 128650. [[CrossRef](#)]
51. Kharbouche, L.; Martínez Galera, M.; Díaz Galiano, F.J.; Gil García, M.D. Pre-concentration of 218 multiclass pesticide in groundwater samples using MSU-1 mesoporous sorbent. *Microchem. J.* **2023**, *184*, 108168. [[CrossRef](#)]
52. Sanchez-Hernandez, L.; Hernandez-Dominguez, D.; Martin, M.T.; Nozal, M.J.; Higes, M.; Yague, J.L.B. Residues of neonicotinoids and their metabolites in honey and pollen from sunflower and maize seed dressing crops. *J. Chromatogr. A* **2016**, *1428*, 220–227. [[CrossRef](#)] [[PubMed](#)]
53. Li, Y.; Long, L.; Ge, J.; Li, H.; Zhang, M.; Wan, Q.; Yu, X. Effect of Imidacloprid Uptake from Contaminated Soils on Vegetable Growth. *J. Agric. Food Chem.* **2019**, *67*, 7232–7242. [[CrossRef](#)] [[PubMed](#)]
54. Li, S.; Li, Z.; Ma, S.; Hao, L.; Liu, W.; Wang, Q.; Wang, C.; Wang, Z.; Wu, Q. Synthesis of nitrogen-rich magnetic hypercrosslinked polymer as robust adsorbent for the detection of neonicotinoids in honey, tomatoes, lettuce and Chinese cabbage. *J. Chromatogr. A* **2022**, *1677*, 463326. [[CrossRef](#)] [[PubMed](#)]
55. Jiang, S.; Meng, X.; Xu, M.; Li, M.; Li, S.; Wang, Q.; Liu, W.; Hao, L.; Wang, J.; Wang, C.; et al. Green synthesis of novel magnetic porous organic polymer for magnetic solid phase extraction of neonicotinoids in lemon juice and honey samples. *Food Chem.* **2022**, *383*, 132599. [[CrossRef](#)]
56. Lu, J.; Wang, R.; Luan, J.; Li, Y.; He, X.; Chen, L.; Zhang, Y. A functionalized magnetic covalent organic framework for sensitive determination of trace neonicotinoid residues in vegetable samples. *J. Chromatogr. A* **2020**, *1618*, 460898. [[CrossRef](#)]
57. Moradi Shahrehabak, S.; Saber-Tehrani, M.; Faraji, M.; Shabanian, M.; Aberoomand-Azar, P. Simultaneous magnetic solid phase extraction of acidic and basic pesticides using triazine-based polymeric network modified magnetic nanoparticles/graphene oxide nanocomposite in water and food samples. *Microchem. J.* **2019**, *146*, 630–639. [[CrossRef](#)]
58. Alizadeh, R.; Mashalavi, B.; Yeganeh Faal, A.; Seidi, S. Development of ultrasound assisted dispersive micro solid phase extraction based on CuO nanoplate-polyaniline composite as a new sorbent for insecticides analysis in wheat samples. *Microchem. J.* **2021**, *168*, 106422. [[CrossRef](#)]
59. Wu, C.; Dong, F.; Mei, X.; Ning, J.; She, D. Isotope-labeled internal standards and grouping scheme for determination of neonicotinoid insecticides and their metabolites in fruits, vegetables and cereals—A compensation of matrix effects. *Food Chem.* **2020**, *311*, 125871. [[CrossRef](#)]
60. Li, H.; Qi, H.; Chang, J.; Gai, P.; Li, F. Recent progress in homogeneous electrochemical sensors and their designs and applications. *TrAC Trends Anal. Chem.* **2022**, *156*, 116712. [[CrossRef](#)]
61. Oliveira, A.E.F.; Bettio, G.B.; Pereira, A.C. Optimization of an Electrochemical Sensor for Determination of Imidacloprid Based on β -cyclodextrin Electropolymerization on Glassy Carbon Electrode. *Electroanalysis* **2018**, *30*, 1929–1937. [[CrossRef](#)]
62. Urbanova, V.; Bakandritsos, A.; Jakubec, P.; Szambo, T.; Zboril, R. A facile graphene oxide based sensor for electrochemical detection of neonicotinoids. *Biosens. Bioelectron.* **2017**, *89*, 532–537. [[CrossRef](#)]
63. Johnson, Z.T.; Williams, K.; Chen, B.; Sheets, R.; Jared, N.; Li, J.; Smith, E.A.; Claussen, J.C. Electrochemical Sensing of Neonicotinoids Using Laser-Induced Graphene. *ACS Sens.* **2021**, *6*, 3063–3071. [[CrossRef](#)]
64. Zhao, Y.; Zheng, X.; Wang, Q.; Zhe, T.; Bai, Y.; Bu, T.; Zhang, M.; Wang, L. Electrochemical behavior of reduced graphene oxide/cyclodextrins sensors for ultrasensitive detection of imidacloprid in brown rice. *Food Chem.* **2020**, *333*, 127495. [[CrossRef](#)] [[PubMed](#)]
65. Guo, J.; Liu, X.; Wang, A.; Yu, X.; Ding, L. Antifouling electrochemical sensor-based on mesoporous silica film for imidacloprid detection in Traditional Chinese medicine. *Microchem. J.* **2022**, *183*, 107964. [[CrossRef](#)]
66. Kumaravel, A.; Chandrasekaran, M. Electrochemical determination of imidacloprid using nanosilver Nafion[®]/nanoTiO₂ Nafion[®] composite modified glassy carbon electrode. *Sens. Actuators B Chem.* **2011**, *158*, 319–326. [[CrossRef](#)]
67. Lezi, N.; Economou, A. Voltammetric Determination of Neonicotinoid Pesticides at Disposable Screen-Printed Sensors Featuring a Sputtered Bismuth Electrode. *Electroanalysis* **2015**, *27*, 2313–2321. [[CrossRef](#)]

68. Nasr-Esfahani, P.; Ensafi, A.A.; Rezaei, B. Fabrication of a highly sensitive and selective modified electrode for imidacloprid determination based on designed nanocomposite graphene quantum dots/ionic liquid/multiwall carbon nanotubes/polyaniline. *Sens. Actuators B Chem.* **2019**, *296*, 126682. [[CrossRef](#)]
69. Lei, W.; Han, Z.; Si, W.; Hao, Q.; Zhang, Y.; Xia, M.; Wang, F. Sensitive and Selective Detection of Imidacloprid by Graphene-Oxide-Modified Glassy Carbon Electrode. *Chemelectrochem* **2014**, *1*, 1063–1067. [[CrossRef](#)]
70. Si, W.; Lei, W.; Hao, Q.; Xia, X.; Zhang, H.; Li, J.; Li, Q.; Cong, R. Facile Synthesis of Nitrogen-doped Graphene Derived from Graphene Oxide and Vitamin B3 as High-performance Sensor for Imidacloprid Determination. *Electrochim. Acta* **2016**, *212*, 784–790. [[CrossRef](#)]
71. Chen, M.; Meng, Y.; Zhang, W.; Zhou, J.; Xie, J.; Diao, G. beta-Cyclodextrin polymer functionalized reduced-graphene oxide: Application for electrochemical determination imidacloprid. *Electrochim. Acta* **2013**, *108*, 1–9. [[CrossRef](#)]
72. Zhang, W.; Liu, C.; Zou, X.; Zhang, H.; Xu, Y. A β -CD/MWCNT-modified-microelectrode array for rapid determination of imidacloprid in vegetables. *Food Anal. Methods* **2019**, *12*, 2326–2333. [[CrossRef](#)]
73. BelBruno, J.J. Molecularly Imprinted Polymers. *Chem. Rev.* **2019**, *119*, 94–119. [[CrossRef](#)] [[PubMed](#)]
74. Rebelo, P.; Costa-Rama, E.; Seguro, I.; Pacheco, J.G.; Nouws, H.P.A.; Cordeiro, M.N.D.S.; Delerue-Matos, C. Molecularly imprinted polymer-based electrochemical sensors for environmental analysis. *Biosens. Bioelectron.* **2021**, *172*, 112719. [[CrossRef](#)] [[PubMed](#)]
75. Ramanavicius, S.; Samukaite-Bubniene, U.; Ratautaite, V.; Bechelany, M.; Ramanavicius, A. Electrochemical molecularly imprinted polymer based sensors for pharmaceutical and biomedical applications (review). *J. Pharm. Biomed. Anal.* **2022**, *215*, 114739. [[CrossRef](#)]
76. Nawaz, N.; Abu Bakar, N.K.; Mahmud, H.N.M.E.; Jamaludin, N.S. Molecularly imprinted polymers-based DNA biosensors. *Anal. Biochem.* **2021**, *630*, 114328. [[CrossRef](#)]
77. Garcia, Y.; Vera, M.; Giraldo, J.D.; Garrido-Miranda, K.; Jimenez, V.A.; Urbano, B.F.; Pereira, E.D. Microcystins Detection Methods: A Focus on Recent Advances Using Molecularly Imprinted Polymers. *Anal. Chem.* **2022**, *94*, 464–478. [[CrossRef](#)]
78. Kong, L.; Jiang, X.; Zeng, Y.; Zhou, T.; Shi, G. Molecularly imprinted sensor based on electropolymerized poly(o-phenylenediamine) membranes at reduced graphene oxide modified electrode for imidacloprid determination. *Sens. Actuators B Chem.* **2013**, *185*, 424–431. [[CrossRef](#)]
79. Zhang, M.; Zhao, H.T.; Xie, T.J.; Yang, X.; Dong, A.J.; Zhang, H.; Wang, J.; Wang, Z.Y. Molecularly imprinted polymer on graphene surface for selective and sensitive electrochemical sensing imidacloprid. *Sens. Actuators B Chem.* **2017**, *252*, 991–1002. [[CrossRef](#)]
80. Tang, F.; Hua, Q.; Wang, X.; Luan, F.; Wang, L.; Li, Y.; Zhuang, X.; Tian, C. A novel electrochemiluminescence sensor based on a molecular imprinting technique and UCNP@ZIF-8 nanocomposites for sensitive determination of imidacloprid. *Analyst* **2022**, *147*, 3917–3923. [[CrossRef](#)]
81. Ma, X.; Pang, C.; Li, S.; Li, J.; Wang, M.; Xiong, Y.; Su, L.; Luo, J.; Xu, Z.; Lin, L. Biomimetic Synthesis of Ultrafine Mixed-Valence Metal-Organic Framework Nanowires and Their Application in Electrochemiluminescence Sensing. *ACS Appl. Mater. Interfaces* **2021**, *13*, 41987–41996. [[CrossRef](#)]
82. Bor, G.; Man, E.; Ugurlu, O.; Ceylan, A.E.; Balaban, S.; Durmus, C.; Pinar Gumus, Z.; Evran, S.; Timur, S. In vitro Selection of Aptamer for Imidacloprid Recognition as Model Analyte and Construction of a Water Analysis Platform. *Electroanalysis* **2020**, *32*, 1922–1929. [[CrossRef](#)]
83. Pérez-Fernández, B.; Mercader, J.V.; Abad-Fuentes, A.; Checa-Orrego, B.I.; Costa-García, A.; Escosura-Muñoz, A.d.l. Direct competitive immunosensor for Imidacloprid pesticide detection on gold nanoparticle-modified electrodes. *Talanta* **2020**, *209*, 120465. [[CrossRef](#)] [[PubMed](#)]
84. Ghodsi, J.; Rafati, A.A. A novel molecularly imprinted sensor for imidacloprid pesticide based on poly(levodopa) electropolymerized/TiO₂ nanoparticles composite. *Anal. Bioanal. Chem.* **2018**, *410*, 7621–7633. [[CrossRef](#)] [[PubMed](#)]
85. Perez-Fernandez, B.; Mercader, J.V.; Checa-Orrego, B.I.; de la Escosura-Muniz, A.; Costa-Garcia, A. A monoclonal antibody-based immunosensor for the electrochemical detection of imidacloprid pesticide. *Analyst* **2019**, *144*, 2936–2941. [[CrossRef](#)]
86. Wei, J.; Liu, C.; Wu, T.; Zeng, W.; Hu, B.; Zhou, S.; Wu, L. A review of current status of ratiometric molecularly imprinted electrochemical sensors: From design to applications. *Anal. Chim. Acta* **2022**, *1230*, 340273. [[CrossRef](#)] [[PubMed](#)]
87. Zhang, J.; Wang, D.; Li, Y. Ratiometric Electrochemical Sensors Associated with Self-Cleaning Electrodes for Simultaneous Detection of Adrenaline, Serotonin, and Tryptophan. *ACS Appl. Mater. Interfaces* **2019**, *11*, 13557–13563. [[CrossRef](#)] [[PubMed](#)]
88. Li, X.; Kan, X. A ratiometric strategy-based electrochemical sensing interface for the sensitive and reliable detection of imidacloprid. *Analyst* **2018**, *143*, 2150–2156. [[CrossRef](#)]
89. Zhang, W.; Liu, C.; Han, K.; Wei, X.; Xu, Y.; Zou, X.; Zhang, H.; Chen, Z. A signal on-off ratiometric electrochemical sensor coupled with a molecular imprinted polymer for selective and stable determination of imidacloprid. *Biosens. Bioelectron.* **2020**, *154*, 112091. [[CrossRef](#)]
90. Tan, G.; Zhao, Y.; Wang, M.; Chen, X.; Wang, B.; Li, Q.X. Ultrasensitive quantitation of imidacloprid in vegetables by colloidal gold and time-resolved fluorescent nanobead traced lateral flow immunoassays. *Food Chem.* **2020**, *311*, 126055. [[CrossRef](#)]
91. Li, H.; Jin, R.; Kong, D.; Zhao, X.; Liu, F.; Yan, X.; Lin, Y.; Lu, G. Switchable fluorescence immunoassay using gold nanoclusters anchored cobalt oxyhydroxide composite for sensitive detection of imidacloprid. *Sens. Actuators B Chem.* **2019**, *283*, 207–214. [[CrossRef](#)]
92. Yu, L.; Song, Z.; Peng, J.; Yang, M.; Zhi, H.; He, H. Progress of gold nanomaterials for colorimetric sensing based on different strategies. *TrAC Trends Anal. Chem.* **2020**, *127*, 115880. [[CrossRef](#)]

93. Sun, J.; Lu, Y.; He, L.; Pang, J.; Yang, F.; Liu, Y. Colorimetric sensor array based on gold nanoparticles: Design principles and recent advances. *TrAC Trends Anal. Chem.* **2020**, *122*, 115754. [[CrossRef](#)]
94. Ma, Y.; Li, Y.; Ma, K.; Wang, Z. Optical colorimetric sensor arrays for chemical and biological analysis. *Sci. China Chem.* **2018**, *61*, 643–655. [[CrossRef](#)]
95. Liu, B.; Zhuang, J.; Wei, G. Recent advances in the design of colorimetric sensors for environmental monitoring. *Environ. Sci. Nano* **2020**, *7*, 2195–2213. [[CrossRef](#)]
96. Yan, P.; Zheng, X.; Liu, S.; Dong, Y.; Fu, T.; Tian, Z.; Wu, Y. Colorimetric Sensor Array for Identification of Proteins and Classification of Metabolic Profiles under Various Osmolyte Conditions. *ACS Sens.* **2023**, *8*, 133–140. [[CrossRef](#)]
97. Tan, S.; Zhao, H.; Tian, D.; Wang, F.; Liu, J.; Li, H. Piperidine–calix [4] arene modified gold nanoparticles: Imidacloprid colorimetric sensing. *Sens. Actuators B Chem.* **2014**, *204*, 522–527. [[CrossRef](#)]
98. Zhao, T.; Liang, X.; Guo, X.; Yang, X.; Guo, J.; Zhou, X.; Huang, X.; Zhang, W.; Wang, Y.; Liu, Z.; et al. Smartphone-based colorimetric sensor array using gold nanoparticles for rapid distinguishment of multiple pesticides in real samples. *Food Chem.* **2023**, *404*, 134768. [[CrossRef](#)] [[PubMed](#)]
99. Wang, S.-H.; Lo, S.-C.; Tung, Y.-J.; Kuo, C.-W.; Tai, Y.-H.; Hsieh, S.-Y.; Lee, K.-L.; Hsiao, S.-R.; Sheen, J.-F.; Hsu, J.-C.; et al. Multichannel nanoplasmonic platform for imidacloprid and fipronil residues rapid screen detection. *Biosens. Bioelectron.* **2020**, *170*, 112677. [[CrossRef](#)]
100. Creedon, N.; Lovera, P.; Moreno, J.G.; Nolan, M.; O’Riordan, A. Highly Sensitive SERS Detection of Neonicotinoid Pesticides. Complete Raman Spectral Assignment of Clothianidin and Imidacloprid. *J. Phys. Chem. A* **2020**, *124*, 7238–7247. [[CrossRef](#)]
101. Sun, Y.; Zhang, N.; Han, C.; Chen, Z.; Zhai, X.; Li, Z.; Zheng, K.; Zhu, J.; Wang, X.; Zou, X.; et al. Competitive immunosensor for sensitive and optical anti-interference detection of imidacloprid by surface-enhanced Raman scattering. *Food Chem.* **2021**, *358*, 129898. [[CrossRef](#)]
102. Zhang, X.; Sun, Z.; Cui, Z.; Li, H. Ionic liquid functionalized gold nanoparticles: Synthesis, rapid colorimetric detection of imidacloprid. *Sens. Actuators B Chem.* **2014**, *191*, 313–319. [[CrossRef](#)]
103. Lee, K.-L.; You, M.-L.; Tsai, C.-H.; Lin, E.-H.; Hsieh, S.-Y.; Ho, M.-H.; Hsu, J.-C.; Wei, P.-K. Nanoplasmonic biochips for rapid label-free detection of imidacloprid pesticides with a smartphone. *Biosens. Bioelectron.* **2016**, *75*, 88–95. [[CrossRef](#)] [[PubMed](#)]
104. Vestri, A.; Rippa, M.; Marchesano, V.; Sagnelli, D.; Margheri, G.; Zhou, J.; Petti, L. LSPR immuno-sensing based on iso-Y nanopillars for highly sensitive and specific imidacloprid detection. *J. Mater. Chem. B.* **2021**, *9*, 9153–9161. [[CrossRef](#)] [[PubMed](#)]
105. Wei, Z.; Zhang, W.; Wang, S.; Han, Y.; Feng, D.; Ma, Y.; Deng, B.; Chen, Z.; Mao, J.; Xu, F.; et al. A ratiometric fluorescent sensor based on molecularly imprinted multilevel mesoporous silica for highly sensitive detection of imidacloprid. *Dyes Pigment.* **2022**, *208*, 110775. [[CrossRef](#)]

Disclaimer/Publisher’s Note: The statements, opinions and data contained in all publications are solely those of the individual author(s) and contributor(s) and not of MDPI and/or the editor(s). MDPI and/or the editor(s) disclaim responsibility for any injury to people or property resulting from any ideas, methods, instructions or products referred to in the content.